ARTICLE

BIOTECHNOLOGY and BIOENGINEERING

# In Vitro Labeling of Hydroxyapatite Minerals by an Engineered Protein

Esra Yuca,[1,2,3] Ayten Yazgan Karatas,[1] Urartu Ozgur Safak Seker,[1] Mustafa Gungormus,[3] Gizem Dinler-Doganay,[1] Mehmet Sarikaya,[1,3] Candan Tamerler[1,3]

[1]Department of Molecular Biology, Genetics and Biotechnology, Istanbul Technical University, Istanbul, Turkey

[2]Department of Biology, Yıldız Technical University, Istanbul, Turkey

[3]Department of Materials Science and Engineering, University of Washington, Roberts Hall, P.O. Box 352120, Seattle, Washington 98195; telephone: 206-543-0724; fax: 206-543-3100; e-mail: candan@u.washington.edu

Received 20 July 2010; revision received 29 November 2010; accepted 9 December 2010

Published online 28 December 2010 in Wiley Online Library (wileyonlinelibrary.com). DOI 10.1002/bit.23041

**ABSTRACT:** Biological and biomimetic synthesis of inorganics have been a major focus in hard tissue engineering as well as in green processing of advanced materials. Among the minerals formed by organisms, calcium phosphate mineralization is studied extensively to understand the formation of mineral-rich tissues. Herein, we report an engineered fusion protein that not only targets calcium phosphate minerals but also allows monitoring of biomineralization. To produce the bi-functional fusion protein, nucleotide sequence encoding combinatorially selected hydroxyapatite-binding peptides (HABP) was genetically linked to the 3′ end of the open reading frame of green fluorescence protein (GFPuv) and successfully expressed in *Escherichia coli*. The fluorescence and binding activities of the bi-functional proteins were characterized by, respectively, using fluorescence microscopy and quartz crystal microbalance spectroscopy. The utility of GFPuv-HABP fusion protein was assessed for both time-wise monitoring of mineralization and the visualization of the mineralized tissues. We used an alkaline phosphatase-based reaction to control phosphate release, thereby mimicking biological processes, to monitor calcium phosphate mineralization. The increase in mineral amount was observed using the fusion protein at different time points. GFPuv-HABP1 was also used for efficient fluorescence labeling of mineralized regions on the extracted human incisors. Our results demonstrate a simple and versatile application of inorganic-binding peptides conjugated with bioluminescence proteins as bi-functional bioimaging molecular probes that target mineralization, and which can be employed to a wide range of biomimetic processing and cell-free tissue engineering.

Biotechnol. Bioeng. 2011;108: 1021–1030.



Correspondence to: Candan Tamerler

Contract grant sponsor: NSF-MRSEC GEMSEC

Contract grant sponsor: TUBITAK/NSF-IRES Joint Project

Contract grant number: 107T250

Contract grant sponsor: SPO project

Additional Supporting Information may be found in the online version of this article.

**KEYWORDS:** hydroxyapatite-binding peptides; green fluorescent protein; mineralization; mineralized tissues; inorganic surfaces; nanobiotechnology

## Introduction

Biomineralization is a process by which organisms produce minerals with controlled hierarchical structures across all dimensional scales from the nanometer and up resulting in superior properties compared to synthetic materials with similar phase compositions (Addadi and Weiner, 1985; Lowenstam, 1981). This topic has attracted major interdisciplinary interest among geologists, biologists, materials scientists, and bioengineers in both the fundamental understanding and mimicking to develop hybrid materials with controlled structures and functions with technological and medical uses. Over 60 different types of minerals, ranging from silicates, carbonates, phosphates, metals to metal oxides, have been identified in organisms (Addadi and Weiner, 1985; Lowenstam, 1981). Hydroxyapatite (HA) has been one of the most extensively studied biominerals, being the principal inorganic component of the hard tissues such as bone and teeth in humans, in particular, and mammals, in general.

The ability to track HA specifically, against the background of other in general calcium phosphates is important in biomedical area, for example, bone and teeth formation/remodeling, gene/drug/cell delivery, regulation of cell bioactivity, and nano-technological implementations, for example, nanoparticle composites (Braux et al., 2009; Dash and Cudworth, 1998; Kasaj et al., 2008; Liu et al., 2005; Ma et al., 2008; Oh et al., 2005; Tan et al., 2007). There are several ways to label calcium orthophosphates both in vivo

and in vitro. The golden standards for in vitro staining of HA are alizarin red S, which stains calcium (Lipman, 1935) and von Kossa stain, which stains phosphates and carbonates (Meloan, 1985). Although frequently used, both of these methods are only applicable in the ex vivo labeling of HA. The methods for potential applications of in vivo HA labeling include synthesizing HA particles doped with fluorescent ions (De Araujo et al., 2007; Yang et al., 2008), synthesizing HA-quantum dot composites (Guo et al., 2008; Hsieh et al., 2009) or modifying the surface of the HA using chemical coupling agents such as bisphosphonates (Zaheer et al., 2001; Zhang et al., 2008). Despite the potentially promising results reported so far, existing methods suffer either from the complex chemistries required for labeling or from the toxicity of the dopants or the composites. Even quantum dots, which have great potential in many research and diagnostic applications, are still considered toxic when they are used in living systems (Alivisatos et al., 2005; Hardman, 2006). Likewise, bisphosphonates, used as a chemical linker, because of their high affinity to hard tissues, carry the risk of disrupting bone turnover due to their inhibitory effects on osteoclasts (Boonekamp et al., 1986; Weinstein et al., 2009).

The green fluorescent protein (GFP) from the bioluminescent jellyfish *Aequorea victoria* has been extensively used as a reporter molecule to monitor expression and localization of many proteins for a wide variety of studies in life sciences (Wang et al., 2009; Zimmer, 2002). There are many recently discovered naturally occurring fluorescent proteins from various marine organisms. Here, we use *Aequorea* GFP, a 238-amino acid long polypeptide with a unique, rigid β-sheet barrel structure. Its enhanced mutants with improved fluorescent properties, have been produced recently (Chudakov et al., 2005; Miyawaki et al., 2005). These variants became commonly used tools in molecular and cellular biology as biological markers due to their robust biological and fluorescence properties (Lippincott-Schwartz and Patterson, 2003). They provide information on detection of the promoter activity, protein localization, motility, and interactions with other proteins in living cells or various cellular parameters in living animals (Chudakov et al., 2005; Hoffman, 2002; Wiedenmann et al., 2009).

The utilization of combinatorial selection techniques such as phage display and cell surface display has recently led to development of a large number of novel peptides that can specifically bind to inorganic substrates. We and other research groups have identified peptide sequences that are specific to a myriad of inorganic materials including noble metals, for example, gold (Brown et al., 2000; Hnilova et al., 2008; Huang et al., 2005), silver (Naik et al., 2002; Nam et al., 2008), and platinum (Seker et al., 2007), oxides, for example, $SiO_2$ (Oren et al., 2007; Tamerler et al., 2007), ZnO (Thai et al., 2004), $Cu_2O$ (Thai et al., 2004), $TiO_2$ (Dickerson et al., 2008; Sano et al., 2005; Sano and Shiba, 2003), minerals HA (Gungormus et al., 2008; Roy et al., 2008), calcite (Gaskin et al., 2000), sapphire (Krauland et al., 2007) and semiconductors [e.g., GaAs (Whaley et al., 2000), ZnS, and CdS (Lee et al., 2002)]. Molecular biology protocols allow further tailoring of the selected solid-binding peptides to improve their affinity and material-selectivity properties so that they can be used in biofunctionalization of nanoparticles and flat substrates (Kacar et al., 2009a; Tamerler et al., 2006). Recently, they have also been used as fusion partners to proteins to develop multifunctional molecular entities for various applications including efficient immobilization of enzymes, nanoparticle synthesis with controlled size (Dai et al., 2005; Kacar et al., 2009b; Kramer et al., 2004; Krauland et al., 2007; Park et al., 2009).

In a previous study, we have reported (phage display selected HA-binding peptides and provided their binding and molecular structural properties (Gungormus et al., 2008). Among these, a high affinity HA-binding heptapeptide, with the amino acid sequence of CMLPHHGAC, was also demonstrated to have mineral-forming capabilities. In the present study, we report a simple and versatile method for fluorescent labeling of this strong hydroxyapatite-binding peptide (HABP1) using a GFP derivative (GFPuv) as a tag and demonstrate its utility as an engineered bi-functional molecular probe for fluorescent labeling of mineralized tissues. The simultaneous formation and labeling of HA were performed in various conditions, including mineral formation on a solid substrate and on existing biological hard tissue as a substrate, to demonstrate its applicability in various biomineralization modalities.

The self-targeting peptide developed here opens up new avenues in the wider utility of combinatorially selected or de novo designed short peptides with inorganic-binding capability as fusion partner to GFPuv. The novel approach provides a robust and versatile molecular probe to monitor inorganics formation in understanding the fundamentals of biomineralization using engineered peptides or tissue-extracted proteins, as well as the assembly and formation of nano-inorganics in more practical technological and medical implementations.

## Materials and Methods

### Genetic Construction of GFPuv and GFPuv-HABP Fusion Proteins

The vector pGFPuv was obtained from Clontech (Takara Bio Inc., Mountain View, CA USA) and used as a template in all polymerase chain reactions (PCR). A GFPuv variant carrying the cycle 3 mutations has an emission maximum at 509 nm and an excitation maximum at 395 nm. The PCR experiments were performed using a high fidelity enzyme, *pfu* DNA polymerase (Fermentas International Inc., Burlington, ON, Canada). All PCR primers used in this study are listed in Table I. Expression vector PQE1 was supplied by Qiagen (Valencia, CA, USA). *E. coli* transformations were performed by electroporation of *E. coli* Top10F' cells with the Eppendorf Electroporator 2510. The DNA sequences of all clones were confirmed via sequencing by using ABI 3300 sequencer with

**Table I.** Primers and their sequences employed in the experiments.

| Primer name | Sequence |
|---|---|
| P1 | 5′-CGGGCATGCTATGAGTAAAGGAGAAGAACTT-3′ |
| P2 | 5′-GCCAAGCTTTTATTTGTAGAGCTCATCCATGCC-3′ |
| P3 | 5′-GCCAAGCTTTTAACAAGCACCATGATGAGGTAACATGCAA CCTCCACCCGATTTGTAGAGCTCATCCATGCC-3′ |
| P4 | 5′-GCCAAGCTTTTAACAAGCACCATGATGAGG-3′ |
| P5 | 5′-GCCAAGCTTTTAACAAGCCTGAGCAAAACCAGGA TTGCAACCTCCACCCGATTTGTAGAGCTCATCCATGCC-3′ |
| P6 | 5′-GCCAAGCTTTTAACAAGCCTGAGCAAAACC-3′ |

P1 forward and P2 reverse primers were used to amplify GFPuv encoding DNA. GFPuv-HABP1 and GFPuv-HABP2 encoding DNA fragments were obtained by overlapping PCR in two steps. In the first step P1–P3 and P1–P5, and in the second step P1–P4 and P1–P6 primers were applied for GFPuv-HABP1 and GFPuv-HABP2, respectively.

BigDye terminator cycle sequencing kit (AB Applied Biosystems Inc., Carlsbad, CA, USA).

GFPuv encoding sequence was amplified using the forward P1 and the reverse P2 primers containing extra residues including a *Pae*I or *Hin*dIII site at their 5′ ends, respectively (Fig. 1a). The DNA fragment encoding GFPuv-fused HABP1 was obtained in a two PCR reactions. The first PCR reaction was kept in 15 cycle and performed by using the forward primer P1 and the reverse primer P3 bearing the strong hydroxyapatite-binding peptide (HABP1) coding sequence with *Hin*dIII cleavage site. The second PCR reaction was kept in 30 cycles and performed by using the forward primer P1 and the reverse primer P4 and the first PCR product as a template. The DNA fragment encoding GFPuv-fused HABP2 was obtained with the same PCR strategy described above using the forward primer P1 and the reverse primer P5 with the control peptide (HABP2) coding sequence with *Hin*dIII cleavage site in the first PCR reaction and the reverse primer P6 in the second PCR reaction. The purified PCR products (Fig. 1b) were ligated into pJET blunt-end PCR cloning vector (Fermentas International Inc.) and then placed into the *Pae*I and *Hin*dIII restriction sites of the expression vector pQE1, which contains an N-terminal 6xHistidine-Tag (Qiagen).

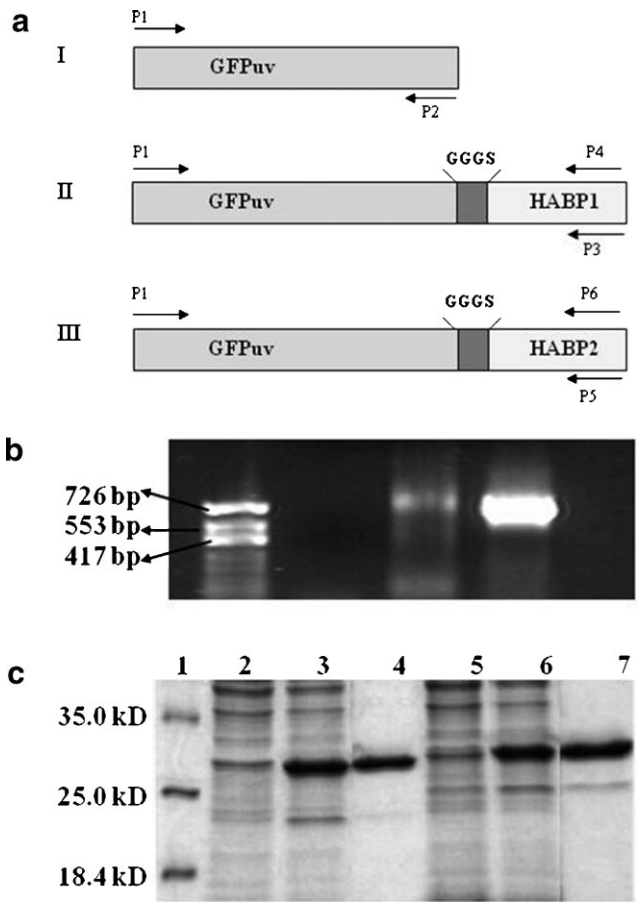


**Figure 1.** **a**: Amplification strategies of (I) GFPuv and (II) GFPuv-HABP1 (III) GFPuv-HABP2. **b**: DNA fragments amplified with *Pfu* DNA polymerase. Lane 1: PhiX174 DNA/HinfI marker 10, lane 2: Negative control, lane 3: Hydroxyapatide-binding peptide-GFPuv encoding DNA fragment, lane 4: GFPuv encoding DNA. **c**: Coomassie blue-stained SDS–PAGE analysis of the *E. coli* lysates. Lane 1: Molecular weight standard, lane 2: Control, uninduced pGFPuv carrying cells, lane 3: pGFPuv carrying cells induced by IPTG, lane 4: Purified GFPuv, lane 5: Control, uninduced pGFPuv-HABP1 carrying cells, lane 6: pGFPuv-HABP1 carrying cells induced with IPTG, lane 7: Purified GFPuv-HABP1.

## Production of Fusion Proteins

Recombinant *E. coli* Top10F' strains (Invitrogen Corporation, Carlsbad, CA, USA) harboring 6His-GFPuv, 6His-GFPuv-HABP1, and 6His-GFPuv-HABP2 expression constructs were grown in LB medium (10 g/Bacto-Tryptone, 5 g/L Bacto-Yeast Extract 10 g/NaCl, pH 7) supplemented with ampicillin (100 μg/mL) at 37°C with shaking at 200 rpm. IPTG (isopropyl-beta-D-thiogalactopyranoside) was then, added at $OD_{600}$ of 0.6 to a final concentration of 1 mM to induce the expression of the target proteins and cultured for an additional 4 h. Cells were harvested by centrifugation at 4,000*g* for 20 min at 4°C and suspended in lysis buffer (50 mM NaH2PO4, 300 mM NaCl, 10 mM imidazole pH 8.0). They were ultrasonicated with a 200 W (six times for 10 s each, keeping the lysate on ice). After centrifugation at 10,000*g* for 20 min at 4°C, the remaining cellular debris was removed. The soluble proteins were applied to molar equivalent amount of $Ni^{2+}$-NTA His-Bind resin (Qiagen) pre-equilibrated with five-column volumes of lysis buffer. After washing with the binding to baseline absorbance, the fusion proteins, having N-terminal 6xHis-tags, were eluted with elution buffer containing 250 mM imidazole. The protein analysis was performed by employing 12% SDS–PAGE (Fig. 1c).

## Fluorescence Microscopy Imaging and Spectrofluorophotometric Analyses

The GFPuv-HABP1, GFPuv-HABP2, and GFPuv expressing cells were monitored using an epifluorescence microscope

(BX60; Olympus Corp., Tokyo, Japan) equipped with a U-MWIB filter cube (Olympus Corp.). Induced culture samples were centrifuged at 5,000*g* for 2 min and the pellets were washed several times with phosphate-buffered saline (PBS) solution (137 mM NaCl, 2.7 mM KCl, 10 mM $Na_2HPO_4$, 2 mM $KH_2PO_4$). The pellets were then gently suspended in PBS solution, and the suspension was deposited on a glass slide to observe the fluorescence activity of the samples. A cooled CCD camera (Diagnostic Instrument, Sterling Heights, MI USA) and Spot Advanced software were used to capture the images of the samples. The excitation, emission wavelengths, and fluorescence properties of the proteins were compared with a control GFPuv using Shimadzu RF-5301 PC spectrofluorophotometer, with the wavelength range of 220–750 nm.

### Binding of GFPuv-HABP Fusion Constructs to Hydroxyapatite

Prior to incubation step, synthetic HA powder (Sigma-Aldrich, St. Louis, MO, USA) was cleaned. A 10-mg powder was suspended in a mixture of 100 μL of distilled water and 900 μL of 1:1 methanol/acetone to remove any organic contaminants. After vortexing, the suspension was sonicated for 20 min in this mixture and then the procedure was repeated in isopropanol. The sonication improves the cleaning by physically removing the contaminants from the surface and dispersing the powder. Next, the powder was washed with phosphate/sodium carbonate (PC) buffer (55 mM $KH_2PO_4$, 45 mM $Na_2CO_3$, 200 mM NaCl pH 7.4) followed by drying in vacuum to remove any organic solvents remaining.

Cleaned HA powder was incubated overnight with purified GFPuv-HABP1 or GFPuv-HABP2, and GFPuv was used as the negative controls at 4 μM concentration in PC buffer containing 0.1% detergent (Tween 20 and 80; Merck, Beeston Nottingham, United Kingdom) at room temperature and with constant rotating using a rotary mixer (Rotator STR4; Stuart Scientific, Staffordshire, United Kingdom) at 20 rpm for 4 h. After the incubation of protein solutions with HA powder, the samples were centrifuged at 200*g* for 3 min at room temperature. The pellets were then washed several times with the same buffer. After removing the supernatant, the GFP-bound HA samples were transferred to a microscope slide and examined under epifluorescence microscope (BX60; Olympus Corp.).

### Secondary Structure Analysis of GFPuv-HABP Constructs

The secondary structure analyses of the constructs were carried out using a Jasco J-810 circular dichroism (CD) spectropolarimeter (Jasco, Easton, MD). The wavelength CD scans were recorded from 200 to 260 nm, and the scan parameters were set at 1-nm step size, 1-nm band width, 50 nm/min speed and 2-s response time. The protein samples of 20 μM were prepared in PC buffer (pH 7), and their CD spectra were measured in the 1-mm path-length CD quartz cuvette (Starna Cells) at room temperature. For each spectrum, three scans were averaged after the background subtraction of the buffer-alone sample. The mean residue molar ellipticity $[\theta_M]$ is expressed in deg × $cm^2$/dmol.

### Quantitative Binding of the Molecular Constructs to HA-Substrate

The quantitative binding of the fusion and wild-type proteins on to HA substrate was carried out using a QCM-D (Quartz Crystal Microbalance with Dissipation Monitoring) system from KSV Instruments (Espoo, Finland), which is equipped with a flow cell and a peristaltic pump. HA-coated QCM-D quartz crystals were used that were purchased from Q-Sense, Frölunda, Q-Sense, Sweden (Switzerland). The crystals were cleaned using 96% (v/v) ethanol and deionized water. The cleaned crystals were mounted in QCM-D instrument and binding properties of the peptides were recorded as a function of time. The protein constructs were prepared in PC buffer at various concentrations of 300, 500, 1,500, and 3,000 nM. The protein solutions were introduced into the chamber of QCM-D in a sequential order, following the baseline equilibration using PC buffer. The kinetics constants were calculated using the frequency change upon adsorption of proteins. Using the dissipation data, we assumed that the proteins form a rigid and dense film on the sensor surface. We used a linear relationship between the deposited mass and frequency based on a viscoelastic film model. The frequency shift was used as a direct signal of the mass adsorbed in the Langmuir adsorption model (see Supporting Information).

### Time-Wise Monitoring of Mineralization on Surfaces

An alkaline phosphatase (AP)-based mineralization model (Gungormus et al., 2008) was used for the formation of mineral layers. This model involves enzymatic hydrolysis of an organic phosphate compound, namely β-Glycerophosphate (β-GP), to $PO_4^{3-}$ by AP. Mineralization solution was prepared using 24 mM $Ca^{+2}$ ($CaCl_2$) and 14.4 mM β-GP in 25 mM Tris–HCl buffer (pH 7.4). When $PO_4^{3-}$ is released to the solution by the action of AP, Ca/P mineralized composition is produced. Following the mineralization reactions, calcium phosphate layers were formed on glass cover slides and samples were examined by optical microscopy using a Nikon Eclipse TE2000-U (Nikon, Melville, NY, USA), scanning electron microscopy (SEM, JSM 7000F JEOL-) and fluorescent microscopy (Nikon Eclipse TE2000-U (Nikon) with fluorescent filters (exciter 460–500, emitter 510–560; Chroma Technology Co, Bellows Falls, VT, USA) at different time intervals, including 0.5, 2, 8, and 24 h. Upon completion of each time interval, the glass slides were taken out and the mineral covered areas on glass slides were determined using Metamorph v7.5 image processing software (Molecular

Devices, Inc., Sunnyvale, CA, USA). The slides were then incubated with 1.4 μM GFPuv and GFPuv-HABP1 (in 24 mM Tris–HCl buffer, pH 7.4). Following a 2-h incubation at room temperature, the slides were rinsed twice in wash buffer containing 0.1% detergent (Tween 20 and 80) and once in Tris–HCl buffer (24 mM; pH: 7.4).

### Labeling Mineralized Tissues In Vitro

Single-rooted teeth, extracted from adult male and female patients, were collected and kept in 70% ethanol (School of Dentistry, Orthodontics Clinic, University of Washington). The specimens were sterilized by ultrasonicating in isopropyl alcohol several times. The ultrasonication also removes any organic remains or calculus from the tooth surface and exposes the mineralized, native surface. Cylindrical pieces were cut from the acellular afibrillar cementum (AAFC), close to the cemento-enamel junction. Prior to incubation with protein samples, cylindrical pieces were examined using an SEM. The teeth sample so prepared were incubated with 1.4 μM GFPuv, GFPuv-HABP1, and GFPuv-HABP2-containing solutions. Upon a 2-h incubation at room temperature, the samples were rinsed twice in wash buffer containing 0.1% detergent and once in 24 mM tris buffer (pH 7.4). The fluorescent microscopy was performed using a Nikon Eclipse TE2000-U (Nikon) microscope and the appropriate fluorescent filter (i.e., exciter 460–500, emitter 510–560; Chroma Technology Co.). The average relative fluorescent intensities were measured in real-time using Metamorph v7.5 image processing software (Molecular Devices).

## Results and Discussion

We engineered a fusion protein encoding both the fluorescence activity of a GFP and the dual, HA-binding and synthesis, activity of a phage display selected heptapeptide. The hypothesis was that the genetic conjugation of GFP to HA-binding peptide would result in a multifunctional molecular probe, which provides targeted labeling and time-wise mineralization monitoring of HA minerals upon fluorescence signal. We demonstrated the applicability of this hypothesis on the synthesized HA mineral on a glass-surface mimicking a solid implant substrate and on a naturally mineralized tissue, namely the root of human incisor teeth, to mimic restoration.

### Production of Recombinant Fusion Proteins

Based on our previous studies with the biocombinatorially selected and characterized HA-binding peptides (Gungormus et al., 2008), a strong-binding (HABP1) and a weak-binding peptide (HABP2) were chosen as fusion partners to GFPuv. We built two different bi-functional constructs: GFPuv-HABP1 and GFPuv-HABP2, and prepared a GFPuv expression construct as control. The plasmids encoding 6His-GFPuv, 6His-GFPuv-HABP1, and 6His-GFPuv-HABP2 fusion proteins were successfully expressed in *E. coli* TOP10 strains and simply purified by using $Ni^{+2}$-chelating resin. The purity and molecular weights of fusion proteins were analyzed by SDS–PAGE (Fig. 1c). The protein bands of GFPuvHABP1, GFPuvHABP2, and GFPuv were, approximately, at 29 kDa compared to theoretical molecular weights, 29.536, 29.478, 28.327, respectively.

### Molecular and Structural Characterization of the GFPuv-HABP Fusion Constructs

Fluorescent properties of the fusion proteins, that is, excitation and emission, were first characterized by fluorescence spectroscopy. We demonstrate that both of the peptide-GFP constructs have equivalent excitation and emission at the same wavelengths with similar intensities as compared to that of GFPuv alone (Fig. 2a). This implies that fluorescence properties of GFPuv were conserved upon the insertion of the designed peptides. Next, the CD spectra

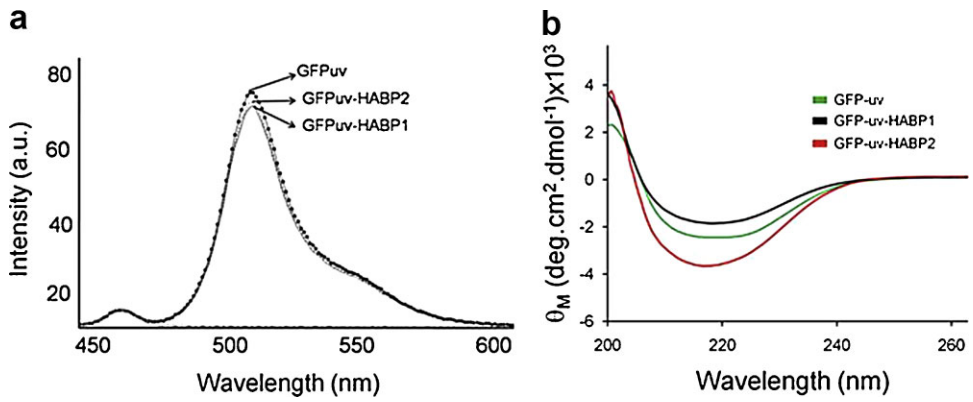


**Figure 2.** **a**: Emission spectra for the purified recombinant proteins. **b**: Secondary structure analysis of GFPuv and GFPuv-HABP constructs using CD, far-UV wavelength scan. [Color figure can be seen in the online version of this article, available at http://wileyonlinelibrary.com/bit]

performed correspond to the dominating β-sheet structure in all cases (Fig. 2b). This results from the presence of the β-barrel core in the GFP that is formed by embedding hydrophobic residues inside and the exposure of hydrophilic residues to the outside of the barrel structure. There is, however, a change in the amount of molar ellipticity possibly revealing a gain, in GFPuv-HABP2, and loss, in GFPuv-HABP1, of protein structure, respectively. However, the variations in the molar ellipticity values by the alteration of GFPuv structure do not correlate with the changes of fluorescence intensities in these constructs, since GFPuv-HABP2 has almost doubled its molar ellipticity value as compared to that of GFPuv. The spatial orientation of the peptide might have caused a slight decrease in the GFPuv fluorescence intensity (Fig. 2a).

The binding properties of fusion proteins to HA surface were also examined. Following the incubation of purified peptides with HA powder, the samples were examined with fluorescent microscopy. The construct with the strong binder sequence, that is, GFPuv-HABP1 fusion, bound to the HA particles with higher affinity than that of the GFPuv-HABP2 or the negative control GFPuv. As demonstrated in our earlier studies, HABP1 and HABP2 were the two peptide sequences presenting similar physicochemical properties but vastly different HA-binding affinities (Gungormus et al., 2008). The results here confirm that the peptides preserved their inorganic-binding properties after being genetically fused to functional proteins. The strong-binding peptide, HABP1, conserves its binding ability without interfering with the GFPuv fluorescence property implying the absence of major intramolecular interactions (Fig. 3).

To test the quantitative-binding characteristics of the constructs, QCM-D studies were carried out using GFPuv, GFPuv-HABP1, and GFPuv-HABP2 and real time adsorptions of the constructs were recorded as a function of time. As shown in Figure 4, the higher amount of protein deposited on the HA-coated QCM-D crystal results in the higher frequency shift. The GFPuv was shown not to bind to HA surface at all. Similarly, the frequency shift that result from the binding of the GFPuv-HABP1 on plain HA surface was detected at a very low level. It is known that GFPuv is a hydrophobic protein (Ishii et al., 2007), and that the HA surface has a high degree of hydrophilicity. The GFP, therefore, is not expected to be adsorbed on the surface of the HA. In the case of the GFPuv-HABP2, the inserted weak binder does not favor the binding of the GFPuv on HA surface, resulting in a limited degree of binding. Moreover, the bound protein is almost desorbed from the HA surface following the washing step. In contrast to the behavior of wild-type GFPuv and GFPuv-HABP2, the bi-functional GFPuv-HABP1 was observed to bind very well on to the HA surface.

The data collected from the QCM-D-binding experiments were utilized to calculate $K_D$ (binding affitinity constant) of the molecular constructs. Simple Langmuir interaction model was used to describe the behavior of

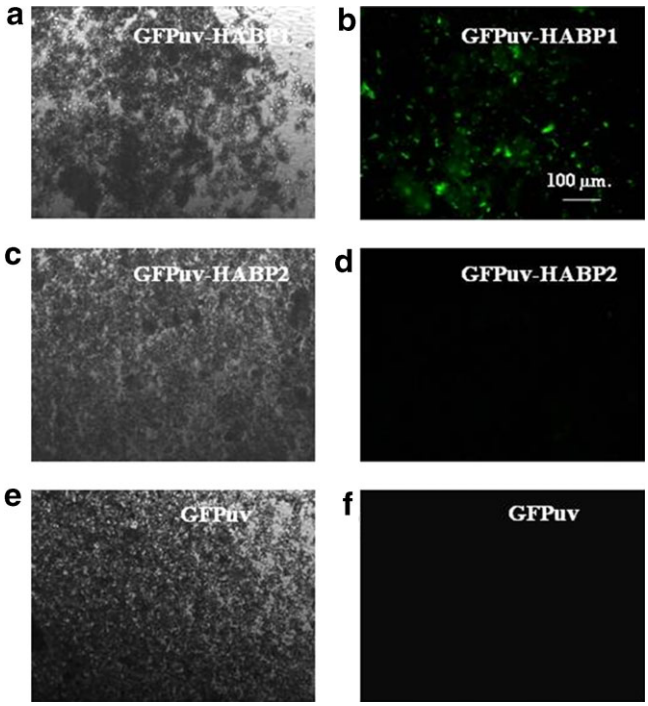


**Figure 3.** Binding characterization of GFPuv, GFPuv-HABP1, and GFPuv-HABP2 proteins on micron-sized HA powders. **a**,**c**,**e**: The bright field images, and (**b**,**d**,**f**) reflects the fluorescence images of the bound proteins, respectively. [Color figure can be seen in the online version of this article, available at http://wileyonlinelibrary.com/bit]

molecular adsorption. Here, the frequency change is related to the adsorbed protein, that is, $\Delta f = (f_{max} \times C)/(K_D + C)$, where $\Delta f$ represents the change in the frequency of the QCM-D at any given protein concentration and $C$ is the corresponding protein concentration. The calculations were carried out for GFPuv-HABP1 and GFPuv-HABP2. To fit the Langmuir model to the experimental data, that is, frequency shift versus protein concentration, the least-squared curve fitting was used and, from these, the $f_{max}$ and $K_D$ values were extracted. As shown from the calculated values, given in Table II, the equilibrium desorption constant of the GFPuv-HABP1 construct ($6.6 \pm 0.3\ \mu M$) is almost 70 times lower than that of the GFPuv-HABP2 ($429 \pm 23\ \mu M$) implying that GFPuv-HABP1 has a higher affinity to the HA substrate. Likewise, the free energy of adsorption ($\Delta G_{abs}$), which is the change in the standard free energy of binding, of GFPuv-HABP1 is higher ($-7$ kcal/mol-K) than that of ($-4.64$ kcal/mol-K). This implies that binding of GFPuv-HABP1 on HA surface is thermodynamically favored compared to GFPuv-HABP2, consequently a high stability in the fusion protein–mineral system is achieved.

### Time-Wise Monitoring Mineralization on Surfaces

The ability of GFPuv-HABP1 construct to monitor the time-wise mineralization was also tested on the HA minerals

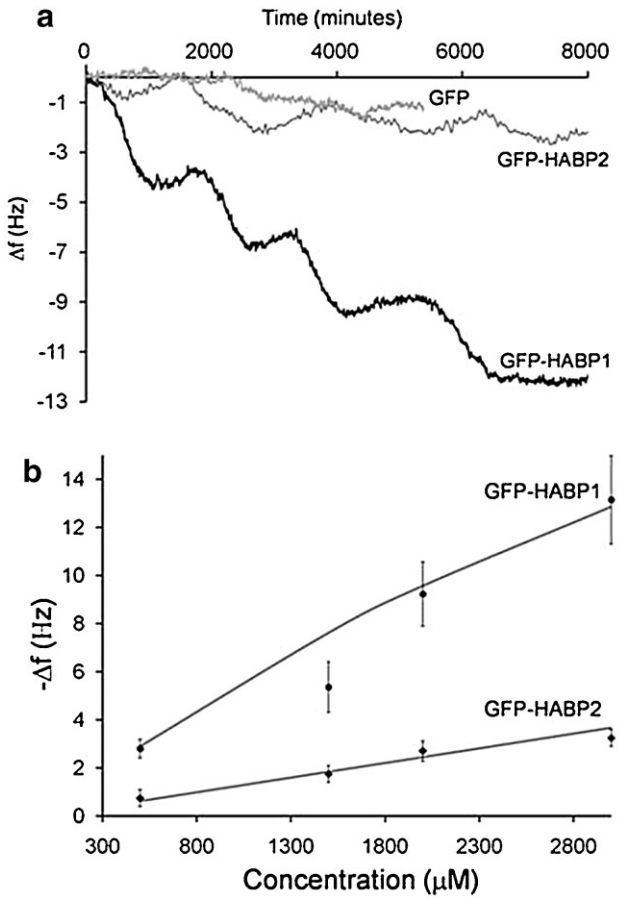


**Figure 4.** **a**: Overall QCM-D sensograms for the adsorption of GFPuv-HABP1, GFPuv-HABP2, and GFPuv on crystalline hydroxyapatite substrates. **b**: The change in QCM-D signal during the adsorption of GFPuv-HABP1 and GFPuv-HABP2 as a function of protein concentration.

formed on glass slides. The imaging experiments using optical microscopy revealed that the amount of mineral on the glass slides increased linearly over time (see Supporting Information). The fluorescent microscopy analysis of the glass slides incubated with GFPuv showed no significant increase in the fluorescent intensity with increasing mineral amount. Since GFPuv lacks the mineral-binding capability, the majority of the GFPuv that was non-specifically bound to the mineral was washed away from the surface upon the rinsing step. On the other hand, the glass slides labeled with GFPuv-HABP1 resulted in an increase in the fluorescent intensity with the increasing mineral amount. These results suggest that the mineral-binding domain of the

**Table II.** The desorption equilibrium ($K_D$) and binding energies ($\Delta G_{abs}$) for GFP-fusion proteins, strong (GFP-HABP1), and weak binder (GFPuv-HABP2).

| Construct | $K_D$ (μM) | $\Delta G$ (kcal/mol) |
|---|---|---|
| GFPuv-HABP1 | $6.6 \pm 0.3$ | $-7.07 \pm 0.30$ |
| GFPuv-HABP2 | $429 \pm 23.5$ | $-4.64 \pm 0.29$ |

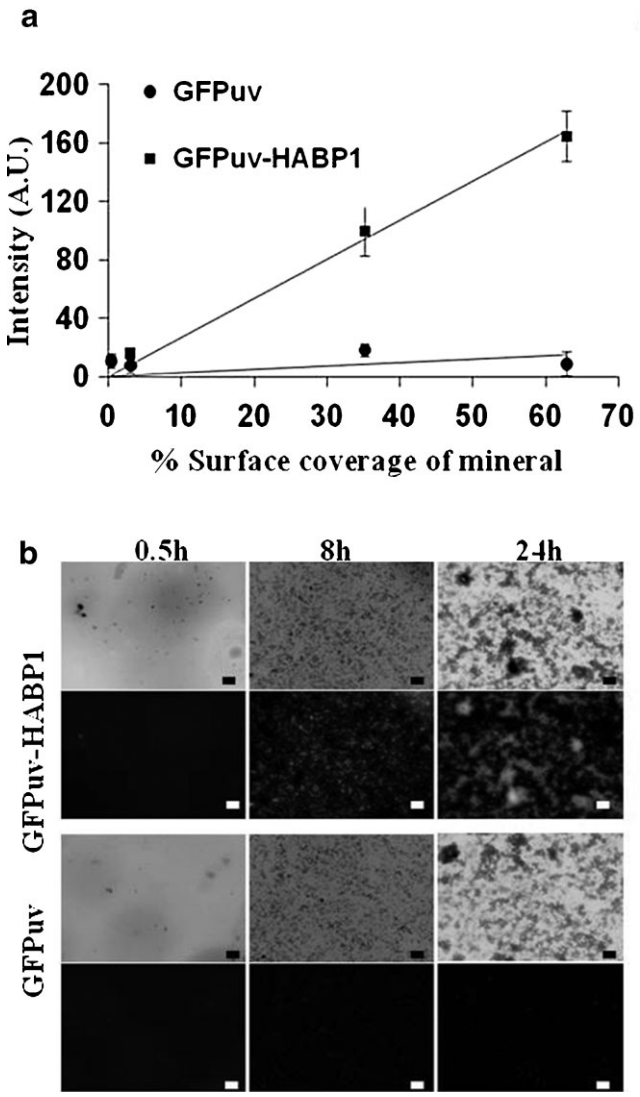


**Figure 5.** **a**: Fluorescent intensity analysis of GFPuv and GFPuv-HABP1 with respect to the increasing mineral coverage on the glass slide. **b**: Fluorescent microscopy images of the minerals produced on the slides over different time points labeled with GFPuv and GFPuv-HABP1.

GFPuv-HABP1 fusion construct facilitates a robust attachment of the GFPuv onto the mineral and prevent desorption even upon a strong washing procedure (Fig. 5). The fluorescent microscopy measurements, in fact, resulted in a linear increase in the intensity versus the amount of mineral formed during the process (Fig. 5a). These results show a semi-quantitative comparison of the protein binding on the HA surface since the roughness and the total surface area of the powder was not accounted for. The approximate surface coverage was rather calculated by comparing the area of the 2D projection of the HA powder in the bright-field image and the area of the 2D projection of the fluorescence image. These results, overall, demonstrate that the GFPuv-HABP1 molecular construct has a potential utility for rapid and accurate monitoring of mineralization of HA in vitro.

### Labeling Mineralized Tissues In Vitro

The binding affinity of the GFPuv-HABP constructs on biological samples was also tested on human AAFC. The acellular cementum consists of a mineralized matrix but lacks collagen fibers and cementocytes. Prior to protein labeling (Fig. 6a), the surface of the root was examined by SEM imaging (Fig. 6b). At identical imaging conditions under the fluorescent microscope, neither of the samples prepared with the incubation of GFPuv or GFPuv-HABP2 displayed any contrast on the teeth surfaces (Fig. 6c and d). Fluorescent contrast, however, was easily discerned on the teeth samples incubated with GFPuv-HABP1, due to its successful attachment to the surfaces (Fig. 6e). The fluorescent images demonstrated that the GFPuv-HABP1 construct can recognize biologically mineralized tissues as well as synthetically formed HA. Fluorescent intensity measurements from the samples indicated that GFPuv-HABP1 yields more than six times higher fluorescent signal on tooth compared to those using either GFPuv or GFPuv-HABP2 (Fig. 6f). Biocombinatorially selected HABPs were reported previously as potential candidates that can bind as well as HA surfaces (Gungormus et al., 2008; Roy et al., 2008; Weiger et al., 2010). Here, they are shown to be effective fusion partners once they are inserted into proteins in order to bring additional functionality to biological and material interface.

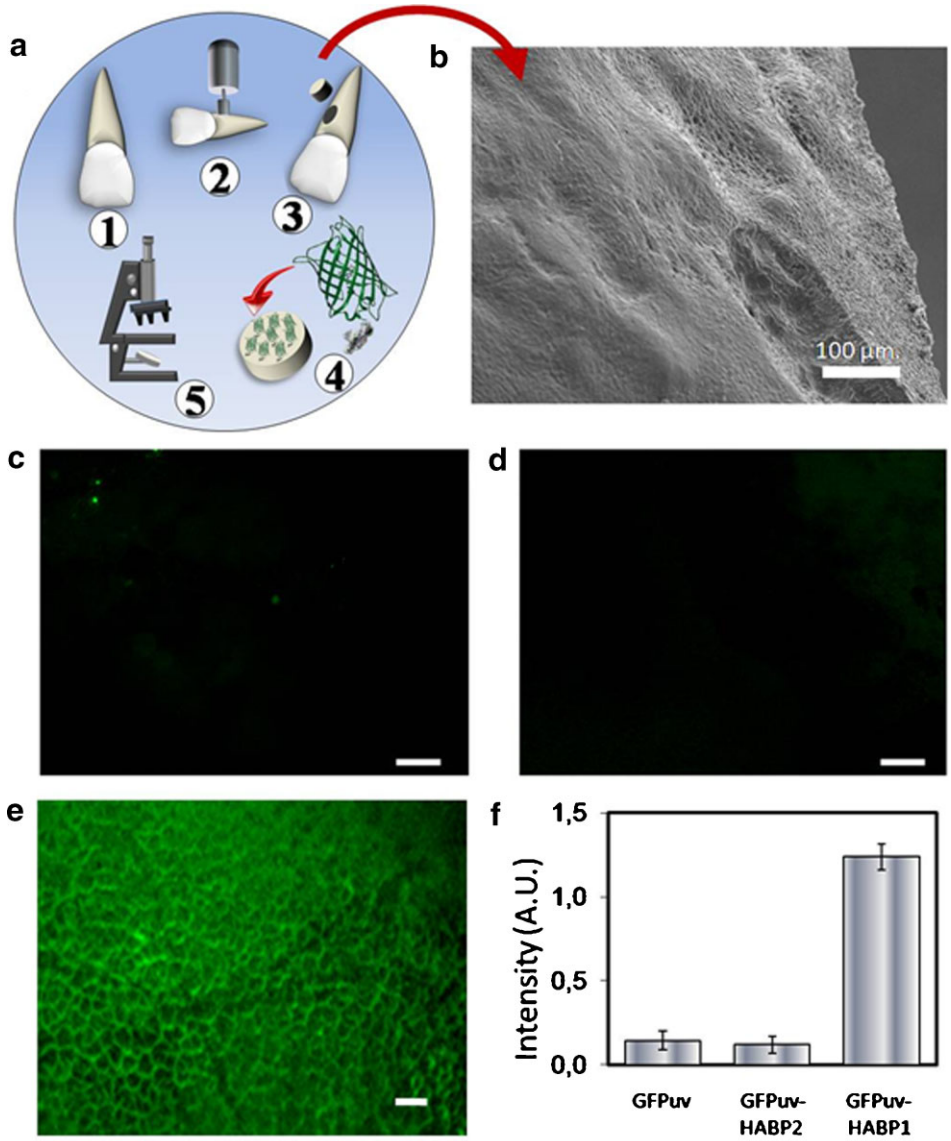


**Figure 6.** **a**: Schematic illustration of the labeling procedure of the teeth samples (1-Extracted human incisors; 2, 3-Cutting cylindrical specimens from the root; 4-Labeling the root surface with the GFPuv-HAPB1; 5-Fluorescent microscopy imaging.). **b**: SEM micrograph of the surface of the root prior to protein labeling. Binding of (**c**) GFPuv, (**d**) GFPuv-HABP2, and (**e**) GFPuv-HABP1 on the cementum of human incisors. **f**: Average fluorescent intensities obtained from the cementum surfaces labeled with GFPuv, GFPuv-HABP2, and GFPuv-HABP1. The values are normalized to the negative control without a protein incubation. [Color figure can be seen in the online version of this article, available at http://wileyonlinelibrary.com/bit]

In summary, a bi-functional fusion protein was successfully produced through a genetic conjugation of mineral-binding peptide and green fluorescent protein. GFPuv-HABP fusion proteins are the first reported set of molecules which can be used to modify and functionalize HA surfaces for biomedical and biotechnological purposes. Besides, the GFPuv-HABP1 construct can serve as an efficient reporter to detect calcium phosphate mineral structures and as an agent for real-time monitoring of in vitro biomineralization processes. The results demonstrated here can be extended to labeling of any mineral or inorganic synthesis by using bi-functional protein conjugates having various inorganic-binding peptides as inserts with potential application areas ranging from fundamental biomimetics processing to restoration and cell-free tissue regeneration.

## Conclusions

Here, we successfully cloned and expressed a fusion protein, GFPuv-HABP1, comprised of a HA-binding peptide with a green fluorescent protein (GFPuv-HABP) as a fluorescence tag. Upon the successful completion of the bi-functional construct, GFPuv-HABP1, the following related questions were posed: Would the molecular structure if the GFP be retained as to provide fluorescence upon genetic fusion of the peptide? Would the solid-binding capability of the peptide be retained?

The structural studies of the cloned, expressed, and purified protein construct revealed that there is some degree of structural rearrangement after the insertion of the HABPs compared to the wild type. The fluorescence properties of the GFPuv, however, were preserved without any significant changes. The quantitative QCM-D binding studies indicated that genetically inserting a HA-binding peptide to GFP-uv had granted it the ability to bind to the mineral surfaces specifically. We demonstrated the versatility of the bio-fluorescence platform produced successfully by carrying out time-wise monitoring of mineralization as well as visualization of biological mineralized tissues. In all cases, GFPuv-HABP1 provided an intense fluorescent labeling on the bound surfaces enabled by the specific inorganic peptide linker.

This is the first time that a bi-functional protein construct was engineered to bind to solid, HA, and fluorescently label the mineral. The novel protein construct GFPuv-HABP1 could potentially be used in a wide variety of applications in biofunctionalization of solid surfaces and monitoring biomineralization. For example, GFPuv-HABP1 could be used for HA formation of surfaces of implants (e.g., titanium), for monitoring tissue regeneration under controlled cell cultures, and for quality control of biomineralization in 3D scaffolds, for example, hydrogels. HA particles conjugated with GFPuv-HABP1 fusion protein have a potential for the utilization of in vitro imaging studies in hard tissue engineering. In general, inorganic-binding peptides genetically conjugated to bioluminescence proteins can be a novel molecular tool for fast screening, labeling and monitoring of minerals, for a wide range of applications in fundamental studies of biomineralization and practical applications in restorative and regenerative medicine. Increasingly, biocombinatorially selected peptides are being demonstrated as enablers for assembly and synthesis of inorganic materials. Using these genetically engineered peptides for inorganics (GEPI), it may be possible to form generic GFPuv-GEPI constructs. The potential for applicability can be then extended to monitoring and probing the formation and utility of nanoparticles and thin films of these materials with useful implementations in nanotechnological and medical sciences.

This work was supported by an NSF-MRSEC GEMSEC (Genetically Engineered Materials Science & Engineering Center) at University of Washington, Seattle, USA and TUBITAK/NSF-IRES Joint Project (107T250), and SPO Project (DPT) at Istanbul Technical University, Turkey.

## References

Addadi L, Weiner S. 1985. Interactions between acidic proteins and crystals—Stereochemical requirements in biomineralization. Proc Natl Acad Sci USA 82(12):4110–4114.

Alivisatos AP, Gu WW, Larabell C. 2005. Quantum dots as cellular probes. Annu Rev Biomed Eng 7:55–76.

Boonekamp PM, Vanderweepals LJA, Vanwijkvanlennep MML, Thesing CW, Bijvoet OLM. 1986. 2 Modes of action of bisphosphonates on osteoclastic resorption of mineralized matrix. J Bone Miner Res 1(1): 27–39.

Braux J, Guillaume C, Jallot E, Nedelec JM, Laurent-Maquin D, Laquerriere P. 2009. Effect of Strontium treatment on human primary osteoblasts. hydroxyapatite: A drug delivery system? Int J Artif Organs 32(7):458–458.

Brown S, Sarikaya M, Johnson E. 2000. A genetic analysis of crystal growth. J Mol Biol 299(3):725–735.

Chudakov DM, Lukyanov S, Lukyanov KA. 2005. Fluorescent proteins as a toolkit for in vivo imaging. Trends Biotechnol 23(12):605–613.

Dai HX, Choe WS, Thai CK, Sarikaya M, Traxler BA, Baneyx F, Schwartz DT. 2005. Nonequilibrium synthesis and assembly of hybrid inorganic-protein nanostructures using an engineered DNA binding protein. J Am Chem Soc 127(44):15637–15643.

Dash AK, Cudworth GC. 1998. Therapeutic applications of implantable drug delivery systems. J Pharmacol Toxicol Methods 40(1):1–12.

De Araujo TS, Macedo ZS, de Oliveira PASC, Valerio MEG. 2007. Production and characterization of pure and $Cr^{3+}$-doped hydroxyapatite for biomedical applications as fluorescent probes. J Mater Sci 42(7):2236–2243.

Dickerson MB, Jones SE, Cai Y, Ahmad G, Naik RR, Kroger N, Sandhage KH. 2008. Identification and design of peptides for the rapid, high-yield formation of nanoparticulate TiO2 from aqueous solutions at room temperature. Chem Mater 20(4):1578–1584.

Gaskin DJH, Starck K, Vulfson EN. 2000. Identification of inorganic crystal-specific sequences using phage display combinatorial library of short peptides: A feasibility study. Biotechnol Lett 22(15):1211–1216.

Gungormus M, Fong H, Kim IW, Evans JS, Tamerler C, Sarikaya M. 2008. Regulation of in vitro calcium phosphate mineralization by combinatorially selected hydroxyapatite-binding peptides. Biomacromolecules 9(3):966–973.

Guo Y, Shi DL, Lian J, Dong ZY, Wang W, Cho HS, Liu GK, Wang LM, Ewing RC. 2008. Quantum dot conjugated hydroxylapatite nanoparticles for in vivo imaging. Nanotechnology 19(17). 6.

Hardman R. 2006. A toxicologic review of quantum dots: Toxicity depends on physicochemical and environmental factors. Environ Health Perspect 114(2):165–172.

Hnilova M, Oren EE, Seker UOS, Wilson BR, Collino S, Evans JS, Tamerler C, Sarikaya M. 2008. Effect of molecular conformations on the adsorption behavior of gold-binding peptides. Langmuir 24(21): 12440–12445.

Hoffman RM. 2002. Green fluorescent protein imaging of tumour growth, metastasis, and angiogenesis in mouse models. Lancet Oncol 3(9):546–556.

Hsieh MF, Li JKJ, Lin CAJ, Huang SH, Sperling RA, Parak WJ, Chang WH. 2009. Tracking of cellular uptake of hydrophilic CdSe/ZnS quantum Dots/Hydroxyapatite composites nanoparticles in MC3T3-E1 osteoblast cells. J Nanosci Nanotechnol 9(4):2758–2762.

Huang Y, Chiang CY, Lee SK, Gao Y, Hu EL, De Yoreo J, Belcher AM. 2005. Programmable assembly of nanoarchitectures using genetically engineered viruses. Nano Lett 5(7):1429–1434.

Ishii M, Kunimura JS, Jeng HT, Vessoni Penna TC, Cholewa O. 2007. Evaluation of the pH- and thermal stability of the recombinant green fluorescent protein (GFP) in the presence of sodium chloride. Appl Biochem Biotechnol 137:555–571.

Kacar T, Ray J, Gungormus M, Oren EE, Tamerler C, Sarikaya M. 2009a. Quartz binding peptides as molecular linkers towards fabricating multifunctional micropatterned substrates. Adv Mater 21(3):295–299.

Kacar T, Zin MT, So C, Wilson B, Ma H, Gul-Karaguler N, Jen AKY, Sarikaya M, Tamerler C. 2009b. Directed self-immobilization of alkaline phosphatase on micro-patterned substrates via genetically fused metal-binding peptide. Biotechnol Bioeng 103(4):696–705.

Kasaj A, Willershausen B, Reichert C, Gortan-Kasaj A, Zafiropoulos GG, Schmidt M. 2008. Human periodontal fibroblast response to a nanostructured hydroxyapatite bone replacement graft in vitro. Arch Oral Biol 53(7):683–689.

Kramer RM, Li C, Carter DC, Stone MO, Naik RR. 2004. Engineered protein cages for nanomaterial synthesis. J Am Chem Soc 126(41): 13282–13286.

Krauland EM, Peelle BR, Wittrup KD, Belcher AM. 2007. Peptide tags for enhanced cellular and protein adhesion to single-crystal line sapphire. Biotechnol Bioeng 97(5):1009–1020.

Lee SW, Mao CB, Flynn CE, Belcher AM. 2002. Ordering of quantum dots using genetically engineered viruses. Science 296(5569):892–895.

Lipman H. 1935. Staining the skeleton of cleared embryos with Alizarin red S. stain. Biotech Histochem 10(2):61–63.

Lippincott-Schwartz J, Patterson GH. 2003. Development and use of fluorescent protein markers in living cells. Science 300(5616):87–91.

Liu TY, Chen SY, Liu DM, Liou SC. 2005. On the study of BSA-loaded calcium-deficient hydroxyapatite nano-carriers for controlled drug delivery. J Control Release 107(1):112–121.

Lowenstam HA. 1981. Minerals formed by organisms. Science 211(4487): 1126–1131.

Ma MY, Zhu YJ, Li L, Cao SW. 2008. Nanostructured porous hollow ellipsoidal capsules of hydroxyapatite and calcium silicate: Preparation and application in drug delivery. J Mater Chem 18(23):2722–2727.

Meloan S, Puchtler H. 1985. Chemical mechanisms of staining methods: von Kossas technique. What von Kossa really wrote and a modified reaction for selective demonstration of inorganic phosphate. J Histotechnol 8:11–13.

Miyawaki A, Nagai T, Mizuno H. 2005. Engineering fluorescent proteins Adv Biochem Eng Biotechnol 95:1–15.

Naik RR, Stringer SJ, Agarwal G, Jones SE, Stone MO. 2002. Biomimetic synthesis and patterning of silver nanoparticles. Nat Mater 1(3):169–172.

Nam KT, Lee YJ, Krauland EM, Kottmann ST, Belcher AM. 2008. Peptide-mediated reduction of silver ions on engineered biological scaffolds. ACS Nano 2(7):1480–1486.

Oh SH, Finones RR, Daraio C, Chen LH, Jin SH. 2005. Growth of nano-scale hydroxyapatite using chemically treated titanium oxide nanotubes. Biomaterials 26(24):4938–4943.

Oren EE, Tamerler C, Sahin D, Hnilova M, Seker UOS, Sarikaya M, Samudrala R. 2007. A novel knowledge-based approach to design inorganic-binding peptides. Bioinformatics 23(21):2816–2822.

Park TJ, Hyun MS, Lee HJ, Lee SY, Ko S. 2009. A self-assembled fusion protein-based surface plasmon resonance biosensor for rapid diagnosis of severe acute respiratory syndrome. Talanta 79(2):295–301.

Roy MD, Stanley SK, Amis EJ, Becker ML. 2008. Identification of a highly specific hydroxyapatite-binding peptide using phage display. Adv Mater 20(10):1830–1836.

Sano KI, Shiba K. 2003. A hexapeptide motif that electrostatically binds to the surface of titanium. J Am Chem Soc 125(47):14234–14235.

Sano KI, Sasaki H, Shiba K. 2005. Specificity and biomineralization activities of Ti-binding peptide-1 (TBP-1). Langmuir 21(7):3090–3095.

Seker UOS, Wilson B, Dincer S, Kim IW, Oren EE, Evans JS, Tamerler C, Sarikaya M. 2007. Adsorption behavior of linear and cyclic genetically engineered platinum binding peptides. Langmuir 23(15):7895–7900.

Tamerler C, Duman M, Oren EE, Gungormus M, Xiong XR, Kacar T, Parviz BA, Sarikaya M. 2006. Materials specificity and directed assembly of a gold-binding peptide. Small 2(11):1372–1378.

Tamerler C, Kacar T, Sahin D, Fong H, Sarikaya M. 2007. Genetically engineered polypeptides for inorganics: A utility in biological materials science and engineering. Mater Sci Eng C 27(3):558–564.

Tan K, Cheang P, Ho IAW, Lam PYP, Hui KM. 2007. Nanosized bioceramic particles could function as efficient gene delivery vehicles with target specificity for the spleen. Gene Ther 14(10):828–835.

Thai CK, Dai HX, Sastry MSR, Sarikaya M, Schwartz DT, Baneyx F. 2004. Identification and characterization of Cu2O- and ZnO-binding polypeptides by Escherichia coli cell surface display: Toward an understanding of metal oxide binding. Biotechnol Bioeng 87(2):129–137.

Wang HX, Nakata E, Hamachi I. 2009. Recent progress in strategies for the creation of protein-based fluorescent biosensors. Chembiochem 10(16):2560–2577.

Weiger MC, Park JJ, Roy MD, Stafford CM, Karim A, Becker ML. 2010. Quantification of the binding affinity of a specific hydroxyapatite binding peptide. Biomaterials 31(11):2955–2963.

Weinstein RS, Roberson PK, Manolagas SC. 2009. Giant osteoclast formation and long-term oral bisphosphonate therapy. N Engl J Med 360(1): 53–62.

Whaley SR, English DS, Hu EL, Barbara PF, Belcher AM. 2000. Selection of peptides with semiconductor binding specificity for directed nanocrystal assembly. Nature 405(6787):665–668.

Wiedenmann J, Oswald F, Nienhaus GU. 2009. Fluorescent proteins for live cell imaging: Opportunities, limitations, and challenges. IUBMB Life 61(11):1029–1042.

Yang P, Quan Z, Li C, Kang X, Lian H, Lin J. 2008. Bioactive, luminescent and mesoporous europium-doped hydroxyapatite as a drug carrier. Biomaterials 29(32):4341–4347.

Zaheer A, Lenkinski RE, Mahmood A, Jones AG, Cantley LC, Frangioni JV. 2001. In vivo near-infrared fluorescence imaging of osteoblastic activity. Nature Biotechnol 19(12):1148–1154.

Zhang Y, Yuan Y, Liu CS. 2008. Fluorescent labeling of nanometer hydroxyapatite. J Mater Sci Technol 24(2):187–191.

Zimmer M. 2002. Green fluorescent protein (GFP): Applications, structure, and related photophysical behavior. Chem Rev 102(3):759–781.